Regular Article

HEMATOPOIESIS AND STEM CELLS

Hematopoietic stem cells develop in the absence of endothelial *cadherin 5* expression

Heidi Anderson,[1,2,*] Taylor C. Patch,[1,*] Pavankumar N. G. Reddy,[2,3] Elliott J. Hagedorn,[2,3] Peter G. Kim,[3] Kathleen A. Soltis,[1] Michael J. Chen,[2,3] Owen J. Tamplin,[2,3] Maike Frye,[4] Glenn A. MacLean,[2,3] Kathleen Hübner,[1] Daniel E. Bauer,[2,3,5] John P. Kanki,[6] Guillaume Vogin,[1] Nicholas C. Huston,[1] Minh Nguyen,[3] Yuko Fujiwara,[2,3] Barry H. Paw,[1-3] Dietmar Vestweber,[4] Leonard I. Zon,[2,3,5,7] Stuart H. Orkin,[2,3,5-7] George Q. Daley,[2,3,5,7] and Dhvanit I. Shah[1,2,5]

[1]Division of Hematology, Department of Medicine, Brigham and Women's Hospital, Boston, MA; [2]Harvard Medical School, Boston, MA; [3]Division of Hematology/Oncology, Boston Children's Hospital, Boston, MA; [4]Max Planck Institute for Molecular Biomedicine, Münster, Germany; [5]Harvard Stem Cell Institute, Cambridge, MA; [6]Department of Pediatric Oncology, Dana-Farber Cancer Institute, Boston, MA; and [7]Howard Hughes Medical Institute, Boston, MA

Key Points

- HSCs emerge, engraft, and differentiate in the absence of *cdh5*.
- HSCs emerging from Cdh5$^{-/-}$ GFP$^{+/+}$ endothelium of mouse chimeric embryos are functional.

Rare endothelial cells in the aorta-gonad-mesonephros (AGM) transition into hematopoietic stem cells (HSCs) during embryonic development. Lineage tracing experiments indicate that HSCs emerge from cadherin 5 (Cdh5; vascular endothelial–cadherin)$^{+}$ endothelial precursors, and isolated populations of Cdh5^{+} cells from mouse embryos and embryonic stem cells can be differentiated into hematopoietic cells. Cdh5 has also been widely implicated as a marker of AGM-derived hemogenic endothelial cells. Because *Cdh5*$^{-/-}$ mice embryos die before the first HSCs emerge, it is unknown whether Cdh5 has a direct role in HSC emergence. Our previous genetic screen yielded *malbec* (*mlb*^{bw306}), a zebrafish mutant for *cdh5*, with normal embryonic and definitive blood. Using time-lapse confocal imaging, parabiotic surgical pairing of zebrafish embryos, and blastula transplantation assays, we show that HSCs emerge, migrate, engraft, and differentiate in the absence of *cdh5* expression. By tracing Cdh5$^{-/-}$green fluorescent protein (GFP)$^{+/+}$ cells in chimeric mice, we demonstrated that Cdh5$^{-/-}$GFP$^{+/+}$ HSCs emerging from embryonic day 10.5 and 11.5 (E10.5 and E11.5) AGM or derived from E13.5 fetal liver not only differentiate into hematopoietic colonies but also engraft and reconstitute multilineage adult blood. We also developed a conditional mouse *Cdh5* knockout (*Cdh5*$^{flox/flox}$*:Scl-Cre-ER*^{T}) and demonstrated that multipotent hematopoietic colonies form despite the absence of *Cdh5*. These data establish that Cdh5, a marker of hemogenic endothelium in the AGM, is dispensable for the transition of hemogenic endothelium to HSCs. (*Blood*. 2015;126(26):2811-2820)

Introduction

During fetal development, rare aortic endothelial cells of the aorta-gonad mesonephros (AGM) region, termed hemogenic endothelial cells, transition to hematopoietic stem cells (HSCs). In zebrafish, the first definitive HSCs emerge from AGM between 30 and 36 hours postfertilization (hpf) and peak at 36 to 72 hpf. These HSCs migrate to caudal hematopoietic tissue (CHT) and later to kidney marrow and thymus.[1] Similarly, adult-type definitive HSCs first emerge in the aortic endothelium of the mouse AGM at embryonic day 10.5 (E10.5) and enter into circulation to seed the fetal liver where the production of hematopoietic progenitor cells occurs. Then, hematopoiesis shifts to the bone marrow and spleen, and the liver becomes the hub of metabolism.[1] Lineage tracing experiments have revealed that HSCs emerge from cadherin 5^{+} (Cdh5^{+}) endothelial precursors.[2,3] Isolated populations of Cdh5^{+} cells from the E11.5 AGM of both murine embryos and mouse embryonic stem (mES) cells differentiate into hematopoietic cells.[4-7] Thus, Cdh5 is a marker of AGM-derived hemogenic endothelial cells transitioning to HSCs.

Sca1, Runx1, and Cdh5 are all markers of HSCs that emerge from hemogenic endothelial cells. Sca1 is itself dispensable for HSC emergence,[8] whereas Runx1 is essential for the formation of erythroid/myeloid progenitors from the yolk sac and HSCs from the hemogenic endothelium.[9] Cdh5, a cell-adhesion molecule, regulates endothelial permeability[10] as well as vascular integrity.[11] Although Cdh5 is present in virtually all active HSCs derived from E11.5 AGM, no difference was observed in multilineage differentiation capacity between vascular endothelial (VE)-cadherin^{+}CD45^{+} and VE-cadherin^{-}CD45^{+} HSCs isolated from the E13.5 liver.[7] In fact, there are conflicting reports suggesting that Cdh5 expression declines either in E13.5 fetal liver[6,7] or in E16.5 fetal liver HSCs.[12] However, there is a consensus that Cdh5 is absent from adult bone marrow HSCs.[6,7,12] Prior studies have established that loss or truncation of *Cdh5* does not significantly impair mouse primitive hematopoiesis in the E8.5 yolk sacs.[13] However, *Cdh5* mutant embryos die at and beyond E9.[13,14] Because HSCs emerge from hemogenic endothelium in the AGM around E10.5,[1,15] the direct role of Cdh5 in endothelial emergence and the development of HSCs as well as in adult hematopoiesis has not yet been firmly established. In this manuscript, we have addressed this question using zebrafish and murine systems.

Submitted July 19, 2015; accepted September 11, 2015. Prepublished online as *Blood* First Edition paper, September 18, 2015; DOI 10.1182/blood-2015-07-659276.

*H.A. and T.C.P. contributed equally to this work, and are co-first authors.

The online version of this article contains a data supplement.

The publication costs of this article were defrayed in part by page charge payment. Therefore, and solely to indicate this fact, this article is hereby marked "advertisement" in accordance with 18 USC section 1734.

Methods

Animal models

All procedures were approved by the animal care and use committee of Boston Children's Hospital. The *malbec* (*mlb*^{bw306}) mutant was recovered from our unbiased chemical mutagenesis screen. C57BL6/J, CD1, and CD45.1 (SJL) mice were purchased from The Jackson Laboratory. Cdh5$^{flox/flox}$ mice were provided by Dietmar Vestweber (Max Planck Institute, Münster, Germany) and Scl-Cre-ER^{T} mice by Stuart H. Orkin (Boston Children's Hospital, Boston, MA).

Mutational analysis and candidate verification

Bioinformatics tools were used to identify and validate *cdh5* as the candidate gene disrupted in the *mlb* locus on the zebrafish chromosome.[16,17] The complementary DNA prepared from wild-type (WT) and *mlb* embryos were sequenced and the mutation in the exon 3 sequence was verified using an allele-specific oligohybridization technique.[18] We performed quantitative reverse transcriptase–polymerase chain reaction (qRT-PCR) using TaqMan gene expression assays (zf-cdh5: Dr03089732_g1 spanning exon 3-4, Dr03089733_m1 spanning exon 4-5, Dr03089737_m1 spanning exon 8-9, Dr03089729_m1 spanning exon 11-12, and zf-hprt: Dr03138604_m1; Applied Biosystems) to measure transcript levels of *cdh5* along the length of the gene. Morpholinos (Gene Tools) against splice sites (TACAAGACCGTCTACCTTTCCAATC) and translational (CCT CCTGGCACACTGTTTCATCATC) sites of *cdh5* were designed and injected into WT embryos to analyze a loss-of-function phenotype. Thirty embryos were pooled in each experiment (n = 5) to isolate RNA for qRT-PCR analysis

Confocal analysis

We crossed *cd41:eGFP*[19] with *flk1:mCherry*[20,21] zebrafish and *runx1+23:NLS-mCherry*[22] with *flk1:eGFP*[23] zebrafish and injected *cdh5*-morpholino in their transgenic embryos. We mounted *cdh5*-silenced transgenic embryos in low-melting-point agarose and used a spinning-disk confocal microscope to perform time-lapse confocal imaging of *cd41:eGFP*$^{+}$ HSCs and *runx1+23:NLS-mCherry*$^{+}$ hematopoietic stem and progenitor cells (HSPCs) emerging from *flk1*$^{+}$ endothelium from 30 to 42 hpf.[22,24] We analyzed 15 *cdh5*-silenced *cd41:eGFP::flk1:mCherry* embryos (vs 13 control) and 23 *cdh5*-silenced *runx1:mCherry::flk1:eGFP* embryos (vs 11 control).

Parabiotic surgery of zebrafish embryos

We injected *cdh5*-morpholino premixed with Dextran blue dye in 1- to 2-cell-stage-old *cd41:eGFP* and *runx1+23:NLS-mCherry* transgenic embryos, and allowed them to grow until their high to 30% epiboly stage. We used custom-made pulled glass needles to fuse the blastula of *cdh5*-silenced transgenic embryos with WT *casper* embryos. We allowed these fused embryos to grow in high-calcium Ringer's solution containing antibiotics, and then tested for the efficacy of fusions 24 hours past surgery.[25] Fused embryos viable after 24 hours of surgery were allowed to grow and were mounted in low-melting-point agarose to test the efficacy of HSC emergence in the morphant embryos. Their migration and engraftment into the WT CHT region between 32 and 48 hpf, and the subsequent differentiation into platelets between days 4 and 5 were captured using confocal microscopes. All 10 of 10 WT parabiots survived whereas 30 of 35 *cdh5*-silenced parabiots survived.

Blastula transplantation assay

We injected *cdh5*-morpholino, premixed with rhodamine-dextran to label all of the donor cells, in *lcr:eGFP* transgenic embryos at the 1-cell stage and allowed them to grow until they were between high or dome stage. We harvested the blastula from *cdh5*-silenced transgenic embryos (donor) and injected ~20 cells into age-matched *WT* embryos (recipient).[26,27] We let these embryos grow, and then tested for *lcr:GFP*$^{+}$ erythroid cells in both morphant and transplanted (recipient) embryos at 36, 48, and 72 hpf (n = 14 recipients).

Electroporation of CRISPR/CAS9 in mouse GFP ES cells

We designed clustered regularly interspaced short palindromic repeat (CRISPR) single guide RNA (sgRNA) sequences flanking exon 1 and exon 12 of the *Cdh5* gene using CRISPR Design software (http://crispr.mit.edu/; supplemental Table 1, see supplemental Data available at the *Blood* Web site). We cloned these sequences in a vector containing Cas9.[28,29] We electroporated the plasmids targeting both the forward and reverse sgRNAs along with the H2B-mKO vector in mouse green fluorescent protein (GFP) embryonic stem (ES) cells (GFP-mESC LB10; GlobalStem) using the GenePulser II (Bio-Rad).[30] We coelectroporated CRISPR constructs with the mH2B-KO vector to allow us to isolate mES cells carrying CAS9, which provides a much greater screening efficiency. We sorted the GFP and orange-positive cells, plated them on mouse embryonic fibroblasts, and genotyped 1869 clones in order to detect a clone containing a homozygous deletion of the *Cdh5* gene using the primers listed in supplemental Table 2.

Karyotyping

We performed karyotyping of candidate *Cdh5*-deleted clones to eliminate a possibility of aneuploidy in their chromosomes during genetic manipulations.[31]

Development of chimeric mice

After engineering mES cells with ubiquitous expression of GFP, and identifying the *Cdh5*$^{-/-}$GFP^{+} mES clone, we karyotyped them to exclude aneuploidy. We injected these Cdh5$^{-/-}$GFP^{+} mES cells (~35-50) into the C57/BL6-derived WT blastocysts to generate chimeric embryos, which were transferred to the oviduct of CD1 foster mothers.[32] Of the 318 injected embryos of 46 foster mothers, 24 chimeric embryos survived up to E11.5 and 11 chimeric embryos survived up to E13.5. In addition, we used 6 E10.5 chimeric embryos to perform immunohistochemistry of Runx1 expression in the AGM region. Extensive detail on numbers of chimeric mice embryos profiled at the E11.5 and E13.5 developmental stage is provided in supplemental Table 3.

Immunohistochemistry

We harvested E10.5 chimeric mouse embryos, embedded them in a paraffin block, performed transverse sections, and immunostained with Runx1, GFP, and 4,6 diamidino-2-phenylindole (DAPI) antibodies in order to detect their expression in the E10.5 AGM region.[33-35]

FACS and CFU analyses

We harvested E11.5 AGM and E13.5 fetal liver tissues from chimeric mouse embryos and used their single-cell suspension for fluorescence-activated cell sorter (FACS), colony-forming unit capacity (CFU), and transplant analyses.[4,33,35] Specifically, we detected expression of GFP, CD41 (phycoerythrin-Cy7), c-Kit (allophycocyanin), CD45.2 (Pacific Blue) in the E11.5 AGM as well as Sca1 (phycoerythrin), c-Kit (allophycocyanin) expression in E13.5 fetal liver. Background staining and negative control for conjugated antibodies are provided in supplemental Figure 8. We also plated 2 embryo equivalent whole E11.5 AGM as well as sorted *Cdh5*-deleted GFP^{+} or sorted control GFP^{-} E13.5 fetal liver cells on M3434 media (StemCell Technologies) and analyzed their capacity to make granulocyte, erythroid, macrophage, megakaryocyte (GEMM), granulocyte macrophage, macrophage, and erythroid colonies.[4,35]

Transplant analysis

We transplanted 2 embryo equivalent (e.e.) chimeric E11.5 whole AGM cells into irradiated (9 cGy, 2 split dose at an interval of 2-3 hours) CD45.1 (SJL) mice. In contrast, we sorted GFP^{+} (Cdh5$^{-/-}$) and GFP^{-} (WT) cells from E13.5 fetal liver cells and transplanted them (~250 000 cells) separately into irradiated CD45.1 mice. We used CD45.1 splenic helper cells for AGM and fetal liver transplants. All GFP^{+} transplants were positive for GFP expression. We then tested the efficiency of these transplanted cells to engraft and reconstitute B cells (CD19), T cells (CD3), and macrophages (Gr1 or Mac1) beginning after 4 weeks of transplantation and up to 16 weeks using FACS analysis.[4,33,35] Extensive detail on numbers of the E11.5 AGM and E13.5 fetal liver transplanted in irradiated SJL mice is provided in supplemental Table 3.

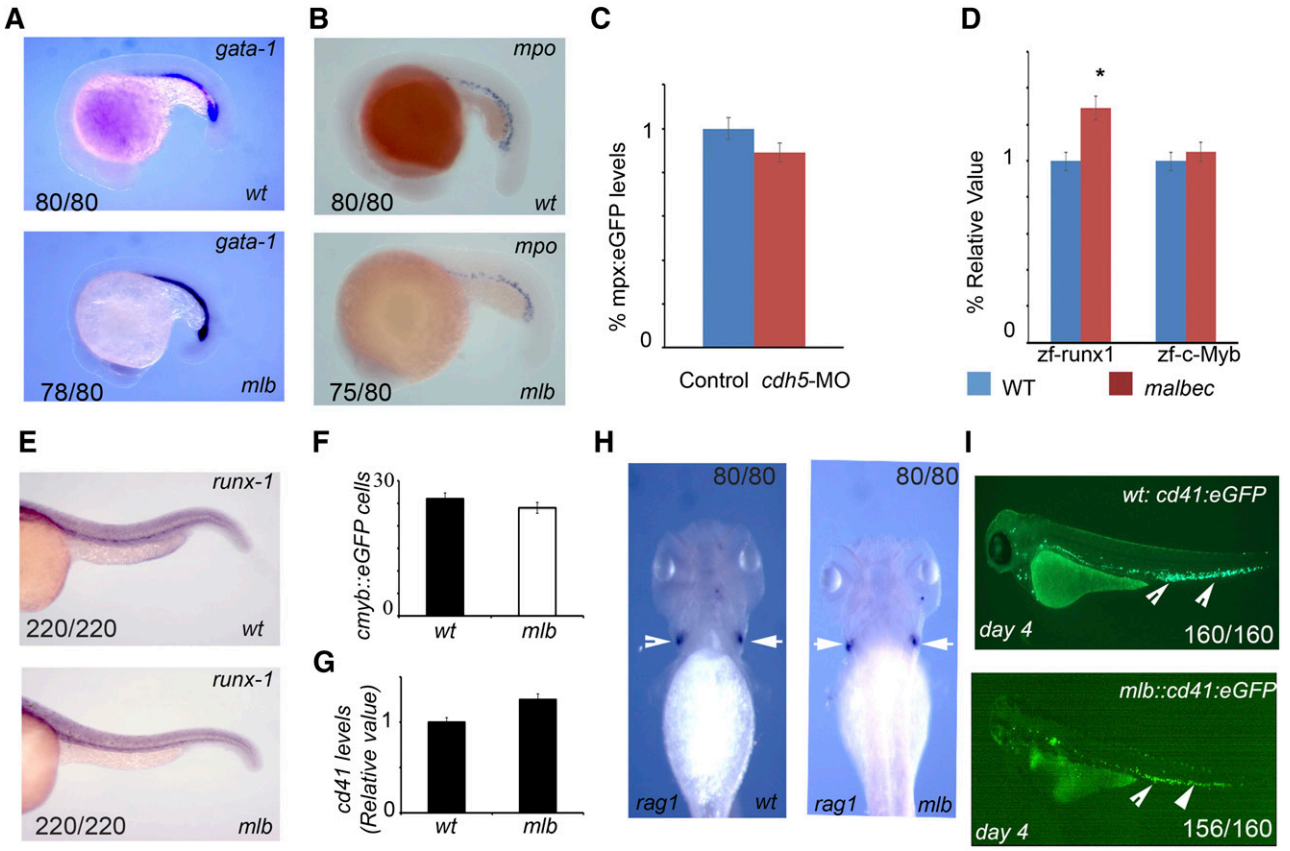

Figure 1. *malbec* (*mlb*^{bw306}) has normal embryonic and definitive hematopoiesis despite disruption of the *cdh5* gene. (A) The expression of *erythro*-myeloid progenitors (gata1) is normal in wt and *mlb* embryos at 20 somite stage (ss). wt: n = 80/80; *mlb*: n = 78/80. (B) WISH analysis of the surrogate marker for myeloid cell expression shows normal *mpo* levels in *mlb* embryos at 20 ss. wt: n = 80/80; *mlb*: n = 75/80. (C) FACS analysis of *mpx:eGFP*$^{+}$ neutrophils in control and *cdh5*-silenced zebrafish embryos. Twenty embryos were used in each experiment; n = 5. (D) qRT-PCR analysis of *runx1* and *c-Myb* mRNA expression in control and *malbec* embryos. Forty embryos were used in each experiment; n = 5. (E) Normal *runx1* mRNA expression in the AGM region of 36-hpf-old wt and *mlb* embryos. wt: n = 220/220; *mlb*: n = 220/220. (F) A progeny of *mlb* crossed with *c-myb:eGFP* has comparable levels of *mlb::c-myb:eGFP*$^{+}$ HSCs cells in *malbec* embryos; n = 60. (G) A progeny of *mlb* crossed with *cd41:eGFP* has comparable levels of *mlb::cd41:eGFP*^{low} HSCs (FACS analysis), indicating that *mlb* produces sufficient amounts of HSCs. Forty embryos pooled in each sample; n = 5. (H) Normal *rag-1* mRNA expression in the thymus of a *mlb* embryo (examples indicated with arrows). wt: n = 80/80; *mlb*: n = 80/80. (I) Progeny of *mlb* crossed with *cd41:eGFP* shows *mlb::cd41:eGFP*$^{+}$ platelets (examples indicated with arrows) at day 4 postfertilization. wt: n = 160/160; *mlb*: n = 156/160. *$P < .05$ (*t* test, error bars indicate standard error of the mean [s.e.m.]).

Development of a conditional *Cdh5* knockout

We developed *Cdh5*$^{flox/flox}$*:Scl-Cre-ER*^{T} (as described in Figure 6A) and verified its genotype (as described in Figure 6B). We injected Tamoxifen (2 mg/kg, subcutaneously [s.c.]) in pregnant *Cdh5*$^{flox/flox}$*:Scl-Cre-ER*^{T} every day from E5.5 to E10.5 (see Figure 6C). At E11.5, we harvested the AGM, seeded its single-cell suspension in M3434 media for CFU analyses, followed by the genotyping of colonies to analyze the *Cdh5* deletion. Sequences for the *Cdh5* and *Cre* primers are listed in supplemental Table 4.

Statistical analyses were performed by Student *t* tests. Significance was set at $P < .05$.

Results

cdh5 is disrupted in the *malbec* locus

To investigate the role of *cadherin* 5 in blood development, we studied *mlb*, an embryonic lethal zebrafish mutant that emerged from an unbiased ethylnitrosourea screen for anemic embryos.[16] We performed chromosomal walking to demonstrate *cadherin 5* (cdh5, VE-CAD) as the most probable candidate gene for the *mlb* locus. To identify the genetic mutation in the *mlb* locus, we sequenced the *cdh5* gene and found an A267T stop codon in exon 3 (supplemental Figure 1A). We then used qRT-PCR (supplemental Figure 1B) and whole-mount in situ hybridization (WISH; supplemental Figure 1C) to validate loss of the *cdh5* messenger RNA (mRNA) levels in *mlb* embryos, suggesting that the A267T stop codon resulted in nonsense-mediated decay of *cdh5* mRNA. As an antibody cross-reacting with zebrafish cdh5 protein was not available, we were unable to directly assay the cdh5 protein levels in *mlb* embryos.

To further verify the loss-of-function phenotype for *cdh5*, we injected 2 independently derived *cdh5* antisense splice-blocking and translational-blocking morpholinos (MOs)[17] to knockdown *cdh5* expression in zebrafish embryos. The *cdh5*-silenced embryos (morphants) phenocopied *mlb*'s anemia (supplemental Figure 1D-E). We further found a loss of *cdh5* mRNA levels in the morphant embryos, suggesting that the splice-blocking MOs accurately targeted *cdh5* (supplemental Figure 1F). Injection of *cdh5* complementary RNA is toxic to *malbec* embryos, so it is not technically feasible to study the gain-of-function phenotype. Our phylogenetic analysis and peptide alignments further demonstrate human (*CDH5*, chromosome 16) and mouse (*Cdh5*, chromosome 8) orthologs for *cdh5* (supplemental Figure 1G). These findings, along with positional cloning, mutational analysis, and qRT-PCR, as well as WISH data provide convincing evidences that *cdh5* is mutated in the *mlb* locus.

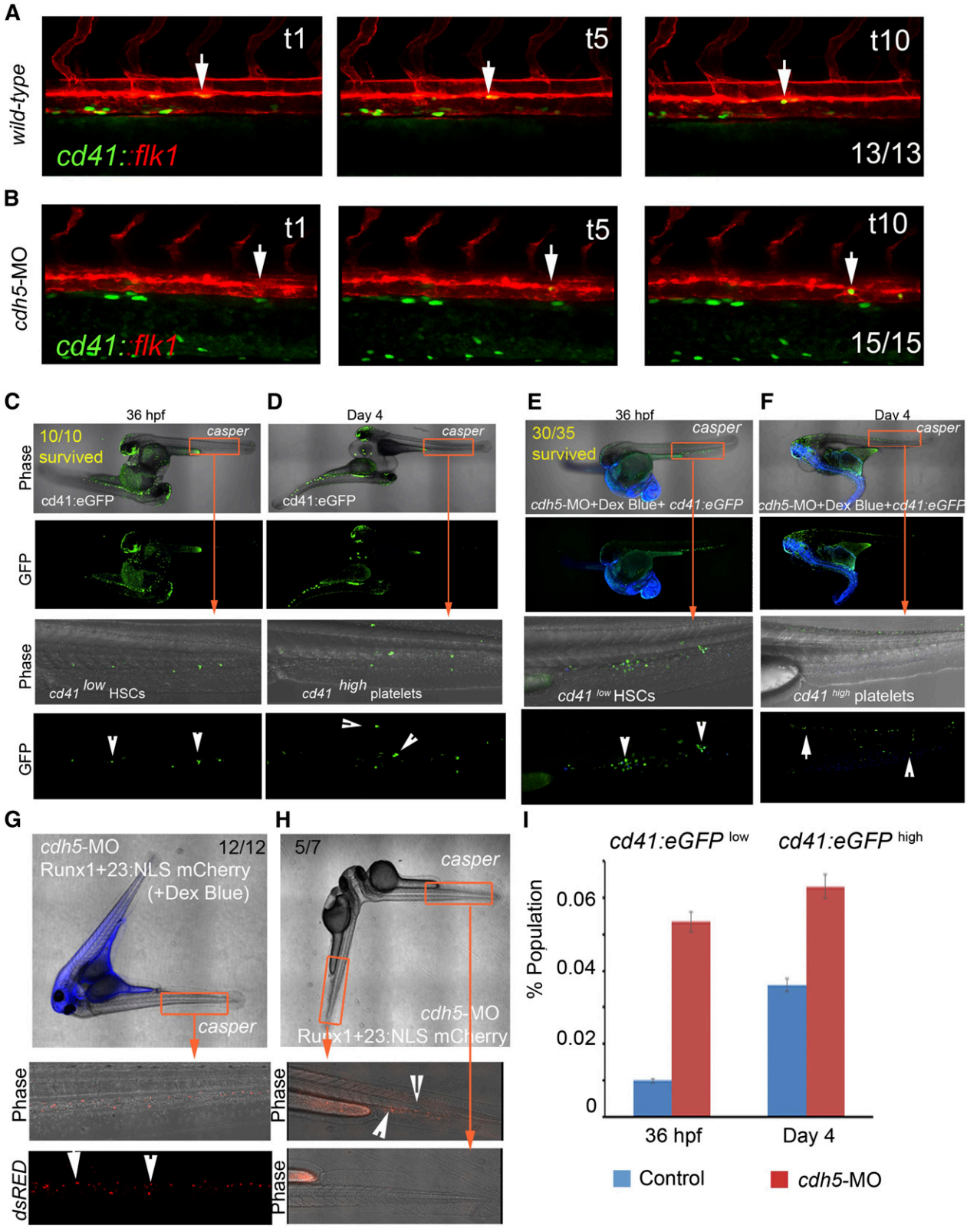

Figure 2. *cdh5* is dispensable for endothelial emergence, migration, engraftment, and differentiation of HSCs. (A) Time-lapse confocal imaging of *cd41:eGFP*$^{+}$ HSCs emerging from *flk1:mCherry*$^{+}$ endothelial cells in control embryos between 30 and 42 hpf (examples are demonstrated with arrows); n = 13/13. (B) *cdh5* silencing in *cd41:eGFP::flk1:mCherry* embryos does not affect endothelial emergence of *cd41:eGFP*$^{+}$ HSCs (examples are demonstrated with arrows); n = 15/15. (C) *cd41:eGFP* transgenic embryo fused to transparent *casper* embryo (wt control) using parabiotic surgery (imaged at 36 hpf), indicates that *cd41:eGFP*^{low} HSCs emerging from the control transgenic embryo migrates to *casper* CHT to engraft and divide (examples are demonstrated with arrows). All 10 of 10 WT parabiots survived. (D) Parabiotic surgery of *cd41:eGFP* transgenic embryo to transparent *casper* embryo shows *cd41:eGFP*^{high} platelets in circulation in transgenic and *casper* embryos (imaged at day 4; examples are demonstrated with arrows). (E) *cdh5*-MO and dextran blue–injected *cd41:eGFP* transgenic embryo fused to transparent *casper* embryo shows the emergence of *cd41:eGFP*^{low} HSCs in *cdh5*-silenced embryo (imaged at 36 hpf), which migrate to *casper* CHT via passive circulation exchange to engraft and further differentiate (examples are

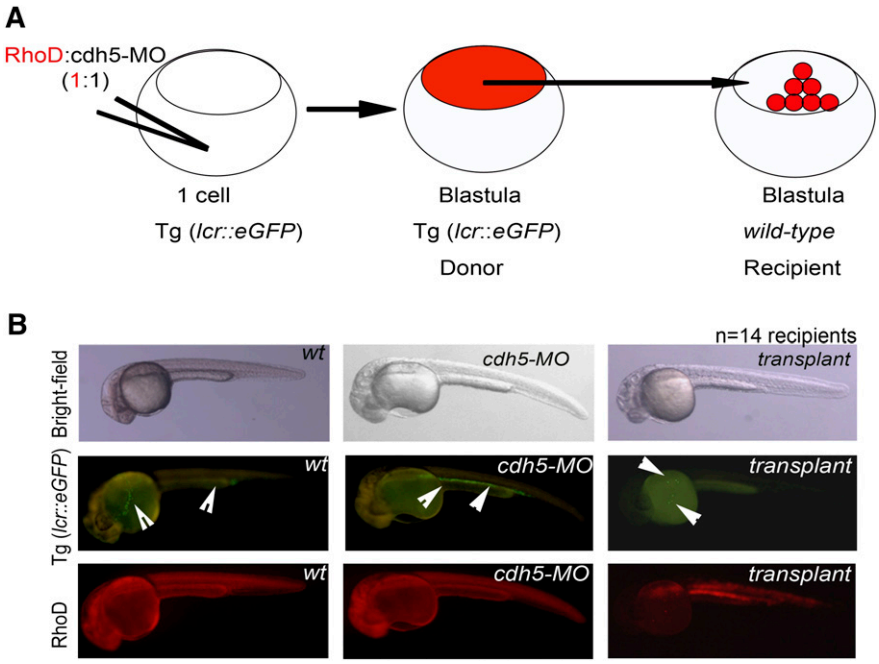

Figure 3. *cdh5*-silenced blastula transplant successfully differentiates into red cells. (A) Schematic representation of the blastula transplantation strategy. Injections of equal amounts of rhodamine and *cdh5*-MO into erythroid transgenic embryo, *lcr:eGFP*, followed by transplantation of *cdh5*-silenced blastula (donor) cells of transgenic embryo between high and dome stage into age-matched *casper*-recipient embryo (wild-type) to analyze whether donor cells can contribute to transgenic erythroid cells in a recipient embryo. (B) Transplantation of *cdh5*-silenced transgenic blastula reconstituted into *lcr:eGFP*$^{+}$ erythroid cells into *casper* recipient embryos, indicating that the cell-intrinsic role of cdh5 is dispensable for blastula differentiation into erythroid cells (examples are demonstrated with arrows); n = 14 recipients.

malbec has normal primitive and definitive blood formation despite circulatory defects

The *cdh5* knockdown zebrafish embryos have impaired cardiac function and circulatory arrest due to poor formation of endocardial junctions, which results in leakage across the endothelial layer and a reduction in the density of the cardiac jelly.[36] We followed the circulation of *lcr:eGFP*$^{+}$ erythroid cells using time-lapse confocal imaging of the *lcr:eGFP::flk1:mCherry* zebrafish embryos between 19 and 32 hpf, and observed no active circulation in *mlb* embryos despite the initiation of a heartbeat. We ruled out necrosis of hematopoietic cells using acridine orange staining of *mlb* embryos (supplemental Figure 2A). We thus concluded that the observed anemic phenotype of *mlb* results from pooling of erythroid cells in blood vessels (supplemental Figure 2B) in the absence of adequate blood circulation.

To study the role of cdh5 in zebrafish hematopoiesis, we first analyzed the expression of markers for primitive and definitive hematopoiesis. Unlike the mouse *Cdh5* mutant, *mlb* zebrafish embryos survive, despite circulatory defects, past the stage when definitive hematopoiesis emerges. We found normal expression of markers for primitive erythroid progenitors (*gata1*) and myeloid (*mpo*, *mpx*) cells in the *mlb* or *cdh5*-MO embryos (Figure 1A-C). Analyzing these markers of definitive hematopoiesis, we detected normal HSCs (*runx1* and *c-Myb* mRNA expression, *mlb*::*c-myb:eGFP*$^{+}$ cells and *mlb*::*cd41:eGFP*^{low} levels) as well as definitive erythroid (*slc4a1*), lymphoid (*rag1*), and thrombocytic (*cd41*) cells (Figure 1D-I; supplemental Figure 2B), indicating that *mlb* has intact primitive and definitive hematopoiesis. Normal expression of *runx1* and *c-myb* (supplemental Figure 2C-E) in *cdh5*-silenced embryos further demonstrates that the *cdh5* morphant phenocopies definitive HSC formation as seen in *mlb*.

HSCs emerge from *cdh5*-silenced hemogenic endothelium

To demonstrate whether HSCs would emerge from *cdh5*-silenced hemogenic endothelium, we first performed time-lapse confocal imaging of *cd41:eGFP*$^{+}$ HSC formation from *flk1:mCherry*$^{+}$ endothelium in zebrafish blood vessels. We found that *cd41:eGFP*$^{+}$ HSCs[19,37] are continuously being formed in the vascular endothelium of the dorsal aorta in *cdh5*-silenced *cd41:eGFP::flk1:mCherry* embryos (Figure 2A-B; supplemental Videos 1-2). We also found that arterial endothelium is intact in *cdh5*-silenced embryos (supplemental Figure 2F). To analyze whether *cd41:eGFP*$^{+}$ HSCs emerging from *cdh5*-silenced *cd41:eGFP*$^{+}$ embryos are null for *cdh5* expression, we sorted *cd41:eGFP*$^{+}$ cells, measured *cdh5* mRNA levels, and found that *cd41:eGFP*$^{+}$ HSCs indeed lack *cdh5* expression (supplemental Figure 2G). These data indicate that arterial endothelium continues to transition to HSCs in the absence of *cdh5*. We independently verified these observations by tracking continuous endothelial emergence of *runx1+23:NLS-mCherry*$^{+}$ HSPCs[22] from *cdh5*-silenced *flk1:eGFP*$^{+}$ vascular endothelium (supplemental Figure 2H-J).

HSCs migrate, engraft, and differentiate in the absence of *cdh5* expression

We performed parabiotic surgery[25] to fuse *cdh5*-silenced *cd41:eGFP* morphant embryos with transparent *casper* embryos, which were otherwise WT. We found that *cd41:eGFP*$^{+}$ HSCs emerged from *cdh5*-silenced aortic endothelium and then migrated to the CHT (a region analogous to mammalian fetal liver) of the *casper* recipients. The *cdh5*-silenced *cd41:eGFP*$^{+}$ HSCs engrafted, divided, and subsequently differentiated into circulating *cd41:eGFP*$^{+}$ platelets at day 4

Figure 2 (continued) demonstrated with arrows). Thirty of 35 *cdh5*-silenced parabiots survived. (F) Four-day-old *cdh5*-silenced *cd41:eGFP* embryo fused to *casper* embryo, indicating that morphant *cd41:eGFP*^{low} HSCs in *casper* CHT differentiated into circulating *cd41:eGFP*^{high} platelets (imaged at day 4; examples with arrows). (G) Surgical fusion of *cdh5*-silenced and dextran blue–injected *runx1+23:NLS-mCherry* with *casper* embryo (imaged at 36 hpf) shows *runx1+23:NLS-mCherry*$^{+}$ HSPCs emerging from *cdh5*-silenced transgenic embryo and engrafting to *casper*'s CHT (examples are demonstrated with arrows). Twelve of 12 parabiots survived. (H) Lateral body-to-head fusion of *cdh5*-silenced *ruxn1+23:NLS-mCherry* embryo with *casper* embryo, showing a lack of circulation exchange between the 2 embryos impedes migration of *cdh5*-silenced *runx1+23:NLS-mCherry*$^{+}$ HSPCs to *casper* (examples are demonstrated with arrows). Five of 7 parabiots survived. (I) Flow analyses of *cd41:eGFP*^{low} HSCs at 36 hpf and *cd41:eGFP*^{high} platelets at day 4 in the control and *cdh5*-silenced *cd41:eGFP* embryos show that differentiation into platelets continues despite the lack of *cdh5*. Twenty embryos were used in each experiment; n = 5. *$P < .05$ (*t* test; error bars indicate s.e.m.).

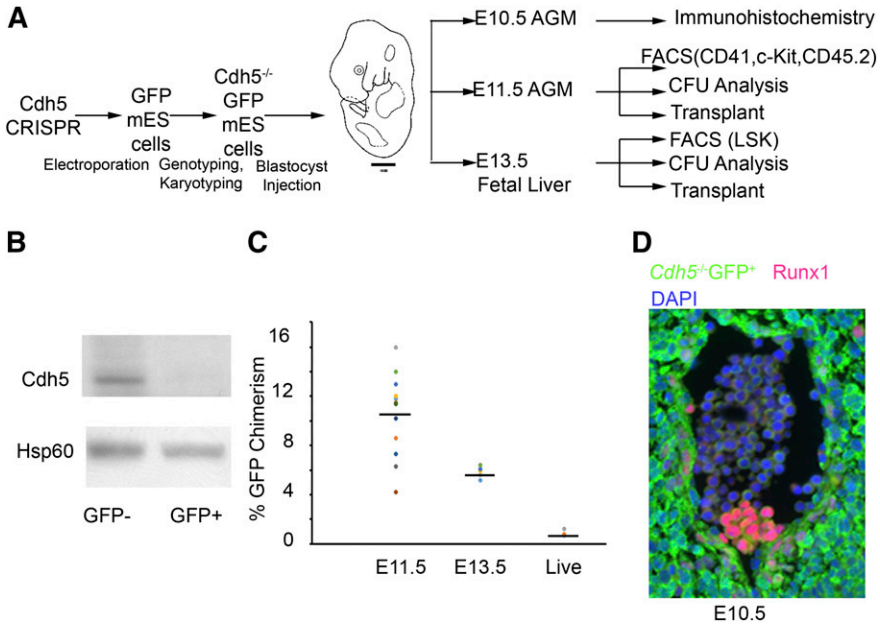

Figure 4. Development and analysis of Cdh5$^{-/-}$GFP$^{+/+}$: Cdh5$^{+/+}$GFP$^{-/-}$ chimeric mice embryos. (A) Schematic representation of the *Cdh5* chimeric mouse development and analysis. Identification of Cdh5$^{-/-}$GFP$^{+/+}$ mES cells after electroporation of *Cdh5* CRISPRs targeting exons 1 to 12 of the *Cdh5* gene followed by karyotyping to exclude aneuploidy. Injection of Cdh5$^{-/-}$GFP^{+} mES cells into WT mouse embryo of foster mothers and harvesting chimeric AGM at E10.5 for immunohistochemistry (GFP, Runx1, DAPI) and at E11.5 for cd41/c-Kit/cd45.2 expression, CFU analysis, transplant into sublethally irradiated mice as well as at E13.5 fetal liver for Lineage^{-}Sca1^{+} c-Kit^{+} expression, CFU analysis, and reconstitution capacity of fetal liver transplants. (B) Western analysis for Cdh5 and Hsp60 protein expression in E13.5 Cdh5$^{-/-}$GFP^{+}: Cdh5$^{+/+}$GFP^{-}-fetal liver–derived GFP^{-} and GFP^{+} cells. To demonstrate the absence of Cdh5 at protein level, we sorted GFP^{+} and GFP^{-} cells from fetal liver of E13.5 *Cdh5*$^{-/-}$ *GFP*$^{+/+}$*:Cdh5*$^{+/+}$ *GFP*$^{-/-}$ chimeric mice embryos. Our western blot data confirmed the absence of Cdh5 protein in GFP^{+} cells. (C) The percentage of GFP chimerism in 11 E11.5 AGM, 6 E13.5 fetal liver, and 3 live pups. (D) Immunostaining of GFP (green), Runx1 (red), and DAPI (violet) in transverse sections of E10.5 AGM region, indicating that Cdh5$^{-/-}$ GFP^{+} cells produced Runx1^{+} GFP^{+} hematopoietic clusters in the ventral wall of the E10.5 dorsal aorta. Magnification, 40×.

postfertilization (Figure 2C-F; supplemental Figure 2G; supplemental Videos 3-4). Similarly, we fused *cdh5*-silenced *runx1+23:NLS-mCherry*$^{+}$ morphant embryos with transparent *casper* embryos, and found that *runx1+23:NLS-mCherry*$^{+}$ HSPCs formed in the *cdh5* morphant embryos migrated to the *casper* WT CHT for engraftment and differentiation (Figure 2G). These data demonstrate that cdh5 is dispensable for HSC formation in the zebrafish, and that *cdh5*-silenced HSCs can migrate, engraft, and differentiate into definitive hematopoietic lineages in a WT hematopoietic niche.

As both *cdh5* morphant and *mlb* mutant embryos have circulation defects, we further analyzed whether the migration of *runx1:mCherry*$^{+}$ HSPCs from *cdh5* morphants to the WT niche was due to a partial recovery of cardiac function and circulation, or due to the exchange of the blastula cells early in development. Because surgically paired embryos appeared to have 1 fused heart, we hypothesized that partial or complete recovery of cardiac function from the WT zebrafish was responsible for the migration of *runx1:mCherry*$^{+}$ HSPCs from *cdh5* morphants to the *casper* niche (Figure 2G). To test this, we fused 2 zebrafish embryos along the lateral body and head, such that the *cdh5* morphant zebrafish could be directly observed to lack active circulation. Indeed, we found that the *runx1: mCherry*$^{+}$ HSPCs could not migrate from *cdh5* morphant to *casper* CHT in these pairs (Figure 2H). These data reinforce the conclusion that *runx1+23:NLS- mCherry*$^{+}$ hematopoietic cells are formed in the AGM of *cdh5* morphant zebrafish embryos and subsequently migrate via passive circulation to the *casper* CHT to engraft and differentiate (Figure 2G-H). We independently verified our time-lapse confocal imaging data by documenting levels of *cd41:eGFP*^{low} HSCs at 36 hpf and their differentiation into *cd41:eGFP*^{high} platelets at day 4 in *cdh5*-morphant embryos (Figure 2I). However, we could not confirm whether the increase in cd41 expression translates into an increase in functional HSCs. Thus, HSCs are being formed in the absence of *cdh5*, and manifest their stem cell properties in a *casper* CHT.

To further investigate the cell-intrinsic roles of cdh5 in HSC differentiation, we silenced *cdh5* in erythroid transgenic *lcr*:eGFP embryos. We then allowed these morphants to develop up to high or dome stage, and then transplanted the blastula cells from *cdh5*-silenced transgenic embryo into WT recipients. We not only found that *cdh5*-morphant embryos produced *lcr:eGFP*$^{+}$ erythroid cells, but also that *cdh5*-silenced blastula transplant (donor) cells contributed to *lcr:eGFP*$^{+}$ erythroid cells in WT recipients at the definitive hematopoiesis stage of embryonic development (Figure 3). These data demonstrate that blastula cells lacking *cdh5* expression differentiate into erythroid cells.

HSC development in *Cdh5*$^{-/-}$*GFP*$^{+/+}$*:Cdh5*$^{+/+}$*GFP*$^{-/-}$ chimeric mice embryos

As *Cdh5* mutant mouse embryos die before first HSCs emerge in AGM, we set out to analyze chimeric mice (in which *Cdh5*$^{-/-}$*GFP*$^{+}$ ES cells injected into *Cdh5*$^{+/+}$*GFP*$^{-}$ blastocysts) to test whether functional HSCs emerge from *Cdh5*-deleted hemogenic endothelium (Figure 4A).

We first used CAS9 nuclease genome editing to target sequences flanking exon 1 and exon 12 of the *Cdh5* gene in mice (supplemental Figure 3A; supplemental Table 1). We engineered mouse ES cells with ubiquitous expression of GFP and identified a *Cdh5*$^{-/-}$GFP^{+} mES clone (supplemental Table 2; supplemental Figure 3B). After verifying loss of *Cdh5* gene expression (supplemental Figure 3B) and confirming their normal karyotype (supplemental Figure 3C), we generated blastocyst chimeras by injecting the *Cdh5*$^{-/-}$*GFP*$^{+}$ mES cells into WT embryos, and then transplanted these chimeric embryos into CD1 foster mothers (Figure 4A). By western blot, we confirmed the absence of Cdh5 expression in GFP^{+} cells isolated by flow cytometric sorting

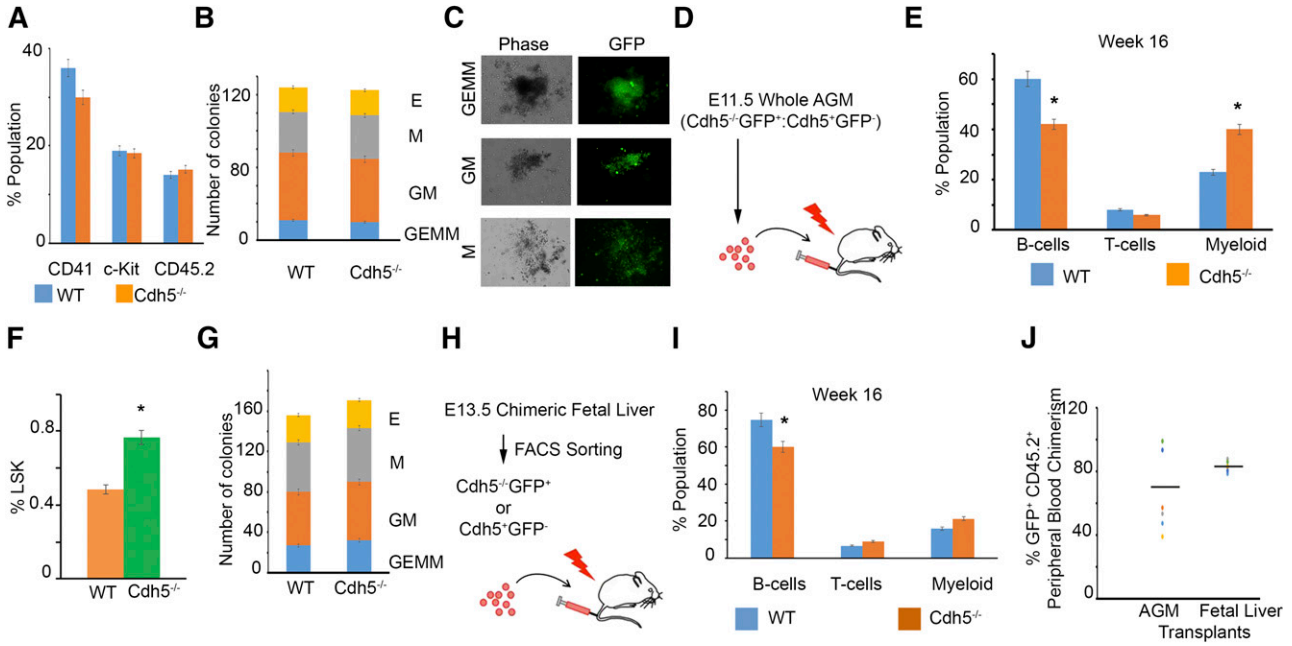

Figure 5. *Cdh5* is dispensable for HSC development in E11.5 AGM and E13.5 fetal liver and reconstitution of multilineage adult hematopoiesis. (A) Quantitative flow analysis of CD41, c-Kit, and CD45.2-positive cells in E11.5 Cdh5$^{-/-}$GFP^{+} and WT (Cdh5$^{+/+}$GFP^{-}) cells, indicating that loss of *Cdh5* is dispensable for CD41, c-Kit, and CD45.2 expression. Eleven AGM were used for FACS analyses. (B) CFU analysis of sorted E11.5 AGM-derived WT and Cdh5$^{-/-}$ GFP^{+} cells, indicating that loss of *Cdh5* has no influence on hematopoietic colony differentiation. Twelve AGM were used for CFU analyses; 2 e.e. per 3.5 mL of M3434 media. (C) Photographs of green fluorescent GFP^{+} hematopoietic colonies formed from the E11.5 AGM-derived Cdh5$^{-/-}$GFP^{+} HSCs. Magnification, ×4. (D) Schema showing the transplant of 2 e.e. E11.5 whole chimeric AGM in irradiated SJL mice. (E) Quantitative analysis of peripheral blood from mice transplanted with 2 e.e. E11.5 chimeric whole AGM, indicating that Cdh5$^{-/-}$GFP^{+} HSCs reconstitute to multilineage adult blood up to 16 weeks of transplant. Twelve AGM were transplanted in 6 SJL recipients. (F) Quantitative analysis of the percentage of Lineage^{-}Sca1^{+}c-Kit^{+} (LSK) cells in WT (Cdh5$^{+/+}$GFP^{-}) and Cdh5$^{-/-}$GFP^{+} compartments of E13.5 fetal liver, indicating that loss of *Cdh5* has no intrinsic influence on development of LSK HSCs. Six fetal livers were used for FACS analyses. (G) CFU analysis of sorted E13.5 fetal liver–derived sorted WT (Cdh5$^{+/+}$GFP^{-}) and Cdh5$^{-/-}$GFP^{+} cells, indicating that loss of *Cdh5* has no influence on hematopoietic colony differentiation. Sorted cells from 10 fetal liver were used for CFU analyses. (H) Schema showing the transplant of E13.5 fetal liver–derived GFP^{+} or GFP^{-} sorted cells in irradiated SJL mice. (I) Quantitative analysis of peripheral blood from mice transplanted with E13.5 fetal liver–derived WT and Cdh5$^{-/-}$GFP^{+} sorted cells, indicating that Cdh5$^{-/-}$GFP^{+} HSCs reconstitute multilineage adult blood up to 16 weeks of transplant; n = 6 recipients. (J) Percentage GFP^{+}CD45.2^{+} peripheral blood chimerism from the Cdh5 knockout cells in E11.5 AGM and E13.5 fetal liver–transplanted recipients. Each dot represents an individual recipient; n = 6; *$P < .05$ (*t* test, error bars indicate s.e.m.).

from the E13.5 fetal livers of chimeric embryos (Figure 4B). The percentage of GFP chimerism in 11 E11.5 AGM, 6 E13.5 fetal liver, and peripheral blood of 3 live pups is provided in Figure 4C.

We recovered E10.5 chimeric embryos, embedded in paraffin, and performed sections. By immunohistochemistry,[33,34] we found that Runx1^{+}GFP^{+} cells emerge from the aortic endothelium (Figure 4D; supplemental Figure 3D-E) in a pattern similar to Runx1^{+} expression in E10.5 WT mice embryos, thus demonstrating the emergence of hematopoietic clusters from *Cdh5*-deleted mammalian hemogenic endothelial cells.

To prove the emergence of functional HSCs, we isolated the AGM from E11.5-old chimeric embryos and analyzed the hematopoietic marker-expression profile, colony formation, and reconstitution capacity of Cdh5$^{-/-}$GFP^{+} or Cdh5$^{+/+}$GFP^{-} AGM-derived cells. These cells expressed CD45.2, c-Kit, and CD41 (Figure 5A; supplemental Figures 4A-D and 5A-D), and differentiated into multipotential GEMM progenitors, granulocyte-macrophage progenitors (CFU-GM, CFU-M, CFU-G), and erythroid colonies (CFU-E) (Figure 5B-C). These data demonstrate that the *Cdh5* is dispensable for CD41, c-Kit, and CD45.2 constitutive expression as well as the hematopoietic colony-forming capacity of Cdh5$^{-/-}$GFP^{+} HSCs. We, however, could not distinguish whether hematopoietic progenitors in E11.5 AGM are from yolk sac or AGM. In addition, transplantation of 2 e.e. of chimeric E11.5 AGM resulted in the long-term (16 week) multilineage engraftment of Cdh5$^{-/-}$GFP^{+} B cells, macrophages, and T cells in irradiated B6.SJL-*Ptprc*^{a} *Pep3*^{b}/BoyJ (CD45.1) recipient mice[4,35] (Figure 5D-E; supplemental Figures 4E-G and 5E-H; Figure 5J).

Similarly, the fetal liver of E13.5 chimeric embryos had Lin^{-}Sca^{+} c-Kit^{+}GFP^{+} hematopoietic cells (Figure 5F; supplemental Figures 6A-C and 7A-C), which differentiated into CFU-GEMM, CFU-GM, CFU-M, and CFU-E hematopoietic colonies (Figure 5G). The transplantation of E13.5 Cdh5$^{-/-}$GFP^{+} or Cdh5$^{+/+}$GFP^{-} fetal liver cells into irradiated CD45.1 mice also produced engraftment with B cells, macrophages, and T cells, indicating production of functional HSCs from *Cdh5*-deficient cells (Figure 5H-I; supplemental Figures 6D-F and 7D-E). To analyze the percentage of donor Cdh5$^{-/-}$GFP^{+} cells contributing to adult lineages, we analyzed the percentage of GFP^{+} CD45.2^{+} peripheral blood chimerism in E11.5 AGM or E13.5 fetal liver transplants (Figure 5J). We also measured the percentage of GFP^{-}CD45.2^{+} peripheral blood chimerism in E11.5 AGM or E13.5 fetal liver transplants to measure WT donor cells contributing to adult lineages (supplemental Figure 7F). To exclude reversion of Cdh5 expression, we also sorted GFP^{+}CD45.2^{+} cells from E13.5 fetal liver transplanted recipients and analyzed Cdh5 gene expression (supplemental Figure 7G). We found deletion of Cdh5 in sorted cells, suggesting that GFP^{+} blood lineages in transplants are derived from *Cdh5*-null GFP^{+} mES cells.

Cdh5 deletion in Scl^{+} cells did not alter hematopoietic colony formation

After generating a conditional mouse *Cdh5* knockout (*Cdh5*$^{flox/flox}$:*Scl-Cre-ER*^{T}; Figure 6A-B), we deleted *Cdh5* floxed alleles beginning at E5.5 using tamoxifen-regulated Cre driven from Scl regulatory sequences. Tamoxifen was injected into pregnant dams from E5.5 to E10.5 to execute

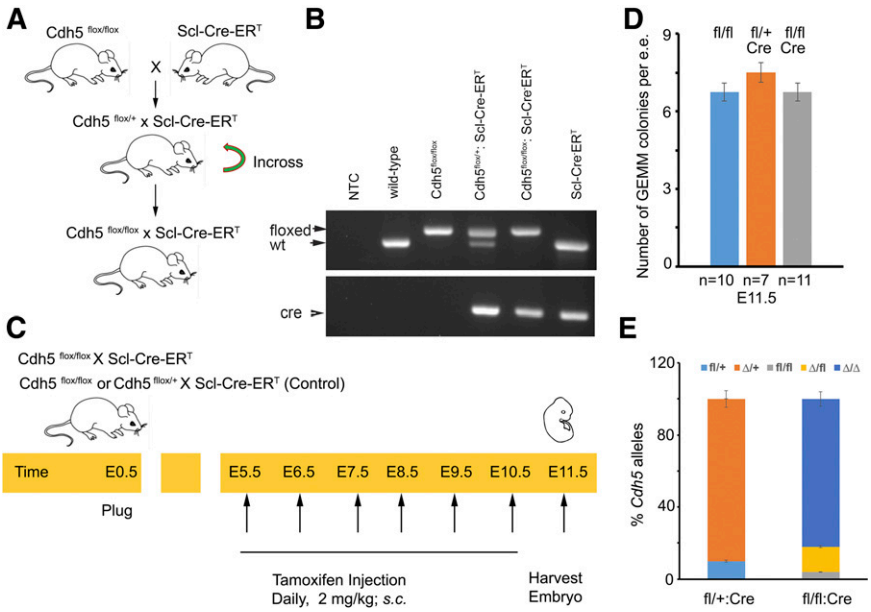

Figure 6. Development of a conditional mouse *Cdh5* knockout. (A) Breeding strategy to develop *Cdh5* $^{flox/flox}$:*Scl-Cre-ER*^{T} mouse. (B) PCR-based strategy to genotype WT, *Cdh5* $^{flox/flox}$, *Cdh5* $^{flox/+}$:*Scl-Cre-ER*^{T}, *Cdh5* $^{flox/flox}$:*Scl-Cre-ER*^{T}, and *Scl-Cre-ER*^{T} using primers listed in supplemental Table 4. (C) Schema to delete *Cdh5* in Scl^{+} cells in *Cdh5* $^{flox/flox}$:*Scl-Cre-ER*^{T}. Tamoxifen was injected in pregnant dam from E5.5 to E10.5 and AGM were harvested on E11.5 for CFU analyses. (D) Average number of GEMM colonies per 1 e.e. AGM derived from Cdh5 $^{flox/flox}$ (n = 10), Cdh5 $^{flox/+}$:Scl-Cre-ER^{T} (n = 7), and Cdh5 $^{flox/flox}$:Scl-Cre-ER^{T} (n = 11), respectively. (E) Percentage Cdh5 alleles in colonies derived from Cdh5 $^{flox/+}$:Scl-Cre-ER^{T} (n = 55 were either fl/+ or Δ/+), and Cdh5 $^{flox/flox}$:Scl-Cre-ER^{T} (n = 72 were fl/fl, Δ/+, or Δ/Δ). *t* test; error bars indicate s.e.m.

the *Cdh5* deletion (Figure 6C). We harvested E11.5 embryos, dissected the AGM, and enumerated CFU colonies in methylcellulose colony-forming assays. We compared the number of GEMM colonies in the *Cdh5*$^{fl/fl}$:*Scl-Cre-ER*^{T} embryos with the *Cdh5*$^{fl/+}$:*Scl-Cre-ER*^{T} embryos for potential Cre toxicity (Figure 6D). We assessed the deletion of the *Cdh5* alleles in individual CFU colonies from *Cdh5*$^{fl/fl}$:*Scl-Cre-ER*^{T} and *Cdh5*$^{fl/+}$:*Scl-Cre-ER*^{T} by PCR (Figure 6E). We found that the deletion of *Cdh5* did not alter numbers of GEMM colonies (Figure 6D). Therefore, Cdh5 is dispensable for hematopoietic colony formation from Scl^{+} cells, further strengthening the conclusion that *Cdh5* is dispensable within blood lineages.

Discussion

Lineage tracing,[2,3] in vitro differentiation,[4,5] and various mouse studies have demonstrated that HSCs emerge from AGM-derived Cdh5^{+} endothelial precursors,[38] implicating Cdh5 as a marker for the hemogenic endothelial cells that transition to HSCs.[39-41] Because *Cdh5* mouse mutant embryos die[13,14] before AGM-derived HSCs emerge at E10.5,[1,15] whether Cdh5 is essential for differentiation of HSCs into definitive blood lineages has remained unclear.[12] In this study, we demonstrate that functional HSCs emerge from *Cdh5*-deficient AGM-hemogenic endothelium during zebrafish and murine fetal development, and show that *Cdh5*-deleted HSCs engraft and reconstitute multilineage adult blood. Thus, we have established that *Cdh5* is dispensable for HSC formation and differentiation (supplemental Figure 9).

Creation of genetic mosaics (chimeras) between WT and genetically modified cells is a well-established and classical strategy for demonstrating cell-intrinsic effects of a gene on cell functions.[42,43] Creation of zebrafish chimeras has been used to study the cell-intrinsic functions of *cloche* and *bloodless* genes in HSPC proliferation, survival, and differentiation.[26,27,44] Here, we demonstrated that transplanted *cdh5*-silenced blastula cells differentiate into red cells in WT zebrafish embryos. To test the cell-intrinsic role of Cdh5 in mammalian blood development and corroborate our findings from zebrafish, we bypassed the lethality of *Cdh5* mutant mouse embryos by creating chimeras of WT mouse embryos with *GFP*$^{+}$*Cdh5*-mutant ES cells. A similar approach has been used to study cell-intrinsic roles of *Ascl2* and *Eed*.[45,46] Although we did not perform comprehensive functional analyses of *Cdh5*-deficient blood cells by competitive transplantation, we observed that *Cdh5*$^{-/-}$*GFP*$^{+}$ cells isolated from E11.5 AGM and E13.5 fetal liver express a normal range of hematopoietic markers, differentiate normally into hematopoietic colonies, and reconstitute normal levels of adult B cells, macrophages, and T cells following transplantation into irradiated SJL mice, indicating the production of functional HSCs from *Cdh5*-deficient cells. We also developed a conditional mouse knockout of *Cdh5* (*Cdh5*$^{flox/flox}$:*Scl-Cre-ER*^{T}) and independently validated that multipotent hematopoietic colonies form from Scl^{+} hemogenic endothelial cells despite the absence of *Cdh5*. Therefore, our zebrafish, mouse chimera, and conditional mouse knockout data demonstrate that although Cdh5 is a marker of definitive hemogenic endothelium, it need not be expressed within the blood lineage to enable HSC emergence and function. However, our data do not exclude the possibility that an unknown molecule might compensate for the function of Cdh5 critical to hematopoietic specification. Our analyses provide a refined view of the molecular features of hemogenic endothelium and illustrate the power of combining model organisms in order to investigate the factors regulating HSC development and differentiation.

Acknowledgments

The authors are grateful to Kathryn Crosier, Philip Crosier, Jeff Cooney, Iman Schultz, Matthew King, Yi Zhou, Christian Lawrence, Eric L. Pierce, Benjanim S. Brigham, Jessica Collantonio, Spencer K. Heggers, and Michelle Cassim for their technical help and/or for providing reagents.

D.I.S. is supported by grants from the American Society of Hematology, the Cooley's Anemia Foundation, and the National Institutes of Health (NIH), National Institute of Diabetes and Digestive and Kidney Diseases (NIDDK) grants (K01DK085217 and R03DK100672). H.A. is supported by a fellowship from the Sigrid Juselius Foundation. E.J.H. is supported by a fellowship from the Helen Hay Whitney Foundation. P.N.G.R. is supported by a fellowship from the American Society of Hematology. O.J.T. is supported by a fellowship from the American Society of Hematology.

G.A.M. is supported by a fellowship from the Alex's Lemonade Stand Foundation. D.E.B. is supported by a grant from the NIH, NIDDK (K08DK093705). B.H.P. is supported by a grant from the NIH, National Heart, Lung, and Blood Institute (P01HL032262). M.F. and D.V. are supported by grants from the Deutsche Forschungsgemeinschaft and the Max Planck Society. L.I.Z. is supported by grants from the NIH National Cancer Institute (R01CA103846) and National Heart, Lung, and Blood Institute (P01HL032262 and R01HL04880). S.H.O. is supported by grants from the NIH NIDDK (P30DK049216) and National Heart, Lung, and Blood Institute (R01HL032259 and P01HL032262). G.Q.D. is supported by grants from the NIH National Heart, Lung and Blood Institute (Progenitor Cell Biology Consortium UO1-HL100001) and NIDDK (R24DK092760), the Alex's Lemonade Foundation, and the Boston Children's Hospital Stem Cell Program.

L.I.Z., S.H.O., and G.Q.D. are investigators of the Howard Hughes Medical Institute.

Authorship

Contribution: D.I.S. originally conceived the project, designed, supervised, and performed the experiments, analyzed data, and wrote the manuscript; H.A. identified the Cdh5 mutation, and performed in situ and blastula transplantation; T.C.P. performed confocal imaging and parabiotic experiments and helped with chimeric mouse experiments; H.A., T.C.P., E.J.H., K.A.S., O.J.T., K.H., N.C.H., J.P.K., and G.V. helped with zebrafish husbandry, imaging, and analyses; T.C.P., P.N.G.R., P.G.K., M.J.C., G.A.M., M.N., and Y.F. helped with mice colony management, injection of mES cells, transplantation of hematopoietic tissues, and FACS analyses; D.E.B. helped to design CRISPR constructs; M.F. and D.V. provided *Cdh5*$^{flox/flox}$ mice; and D.V., B.H.P., L.I.Z., S.H.O., and G.Q.D. analyzed data and wrote the manuscript.

Conflict-of-interest disclosure: The authors declare no competing financial interests.

The current affiliations are: H.A., University of Helsinki, Helsinki, Finland; K.A.S., University of Buffalo School of Medicine and Biomedical Sciences, Buffalo, NY; M.F., Uppsala University, Uppsala, Sweden; K.H., Max Planck Institute for Molecular Biomedicine, Münster, Germany; J.P.K., The Medical Foundation, Boston, MA; and G.V., Institut de Cancerologie de Lorraine, Vandoeuvre-lès-Nancy, France.

Correspondence: Dhvanit I. Shah, Division of Hematology, Brigham and Women's Hospital, Harvard Medical School, Harvard Stem Cell Institute, Boston, MA 02115; e-mail: dshah@research.bwh.harvard.edu.

References

1. Orkin SH, Zon LI. Hematopoiesis: an evolving paradigm for stem cell biology. *Cell.* 2008;132(4):631-644.
2. Zovein AC, Hofmann JJ, Lynch M, et al. Fate tracing reveals the endothelial origin of hematopoietic stem cells. *Cell Stem Cell.* 2008;3(6):625-636.
3. Chen MJ, Yokomizo T, Zeigler BM, Dzierzak E, Speck NA. Runx1 is required for the endothelial to haematopoietic cell transition but not thereafter. *Nature.* 2009;457(7231):887-891.
4. Kim PG, Albacker CE, Lu YF, et al. Signaling axis involving Hedgehog, Notch, and Scl promotes the embryonic endothelial-to-hematopoietic transition. *Proc Natl Acad Sci USA.* 2013;110(2):E141-E150.
5. Fraser ST, Ogawa M, Nishikawa S, Nishikawa S. Embryonic stem cell differentiation as a model to study hematopoietic and endothelial cell development. *Methods Mol Biol.* 2002;185:71-81.
6. Taoudi S, Morrison AM, Inoue H, Gribi R, Ure J, Medvinsky A. Progressive divergence of definitive haematopoietic stem cells from the endothelial compartment does not depend on contact with the foetal liver. *Development.* 2005;132(18):4179-4191.
7. North TE, de Bruijn MF, Stacy T, et al. Runx1 expression marks long-term repopulating hematopoietic stem cells in the midgestation mouse embryo. *Immunity.* 2002;16(5):661-672.
8. Bradfute SB, Graubert TA, Goodell MA. Roles of Sca-1 in hematopoietic stem/progenitor cell function. *Exp Hematol.* 2005;33(7):836-843.
9. Tober J, Yzaguirre AD, Piwarzyk E, Speck NA. Distinct temporal requirements for Runx1 in hematopoietic progenitors and stem cells. *Development.* 2013;140(18):3765-3776.
10. Hordijk PL, Anthony E, Mul FP, Rientsma R, Oomen LC, Roos D. Vascular-endothelial-cadherin modulates endothelial monolayer permeability. *J Cell Sci.* 1999;112(Pt 12):1915-1923.
11. Giannotta M, Trani M, Dejana E. VE-cadherin and endothelial adherens junctions: active guardians of vascular integrity. *Dev Cell.* 2013;26(5):441-454.
12. Kim I, Yilmaz OH, Morrison SJ. CD144 (VE-cadherin) is transiently expressed by fetal liver hematopoietic stem cells. *Blood.* 2005;106(3):903-905.
13. Carmeliet P, Lampugnani MG, Moons L, et al. Targeted deficiency or cytosolic truncation of the VE-cadherin gene in mice impairs VEGF-mediated endothelial survival and angiogenesis. *Cell.* 1999;98(2):147-157.
14. Vittet D, Buchou T, Schweitzer A, Dejana E, Huber P. Targeted null-mutation in the vascular endothelial-cadherin gene impairs the organization of vascular-like structures in embryoid bodies. *Proc Natl Acad Sci USA.* 1997;94(12):6273-6278.
15. Dzierzak E, Speck NA. Of lineage and legacy: the development of mammalian hematopoietic stem cells. *Nat Immunol.* 2008;9(2):129-136.
16. Leshchiner I, Alexa K, Kelsey P, et al. Mutation mapping and identification by whole-genome sequencing. *Genome Res.* 2012;22(8):1541-1548.
17. Shah DI, Takahashi-Makise N, Cooney JD, et al. Mitochondrial Atpif1 regulates haem synthesis in developing erythroblasts. *Nature.* 2012;491(7425):608-612.
18. Kazazian HH Jr, Orkin SH, Markham AF, Chapman CR, Youssoufian H, Waber PG. Quantification of the close association between DNA haplotypes and specific beta-thalassaemia mutations in Mediterraneans. *Nature.* 1984;310(5973):152-154.
19. Ma D, Zhang J, Lin HF, Italiano J, Handin RI. The identification and characterization of zebrafish hematopoietic stem cells. *Blood.* 2011;118(2):289-297.
20. Huang H, Zhang B, Hartenstein PA, Chen JN, Lin S. NXT2 is required for embryonic heart development in zebrafish. *BMC Dev Biol.* 2005;5:7.
21. Chi NC, Shaw RM, De Val S, et al. Foxn4 directly regulates tbx2b expression and atrioventricular canal formation. *Genes Dev.* 2008;22(6):734-739.
22. Tamplin OJ, Durand EM, Carr LA, et al. Hematopoietic stem cell arrival triggers dynamic remodeling of the perivascular niche. *Cell.* 2015;160(1-2):241-252.
23. Cross LM, Cook MA, Lin S, Chen JN, Rubinstein AL. Rapid analysis of angiogenesis drugs in a live fluorescent zebrafish assay. *Arterioscler Thromb Vasc Biol.* 2003;23(5):911-912.
24. Bertrand JY, Chi NC, Santoso B, Teng S, Stainier DY, Traver D. Haematopoietic stem cells derive directly from aortic endothelium during development. *Nature.* 2010;464(7285):108-111.
25. Demy DL, Ranta Z, Giorgi JM, Gonzalez M, Herbomel P, Kissa K. Generating parabiotic zebrafish embryos for cell migration and homing studies. *Nat Methods.* 2013;10(3):256-258.
26. Parker L, Stainier DY. Cell-autonomous and non-autonomous requirements for the zebrafish gene cloche in hematopoiesis. *Development.* 1999;126(12):2643-2651.
27. Ho RK, Kane DA. Cell-autonomous action of zebrafish spt-1 mutation in specific mesodermal precursors. *Nature.* 1990;348(6303):728-730.
28. Yang H, Wang H, Jaenisch R. Generating genetically modified mice using CRISPR/Cas-mediated genome engineering. *Nat Protoc.* 2014;9(8):1956-1968.
29. Wu X, Scott DA, Kriz AJ, et al. Genome-wide binding of the CRISPR endonuclease Cas9 in mammalian cells. *Nat Biotechnol.* 2014;32(7):670-676.
30. Canver MC, Bauer DE, Dass A, et al. Characterization of genomic deletion efficiency mediated by clustered regularly interspaced palindromic repeats (CRISPR)/Cas9 nuclease system in mammalian cells. *J Biol Chem.* 2014;289(31):21312-21324.
31. Bronson SK, Smithies O, Mascarello JT. High incidence of XXY and XYY males among the offspring of female chimeras from embryonic stem cells. *Proc Natl Acad Sci USA.* 1995;92(8):3120-3123.
32. Nagy A, Gertsenstein M, Vintersten K, Behringer R. Manipulating the Mouse Embryo: A Laboratory

Manual. Cold Spring Harbor, NY: Cold Spring Harbor Laboratory Press; 2003.

33. Chen MJ, Li Y, De Obaldia ME, et al. Erythroid/myeloid progenitors and hematopoietic stem cells originate from distinct populations of endothelial cells. *Cell Stem Cell.* 2011;9(6):541-552.
34. Yokomizo T, Yamada-Inagawa T, Yzaguirre AD, Chen MJ, Speck NA, Dzierzak E. Whole-mount three-dimensional imaging of internally localized immunostained cells within mouse embryos. *Nat Protoc.* 2012;7(3):421-431.
35. Arora N, Wenzel PL, McKinney-Freeman SL, et al. Effect of developmental stage of HSC and recipient on transplant outcomes. *Dev Cell.* 2014;29(5):621-628.
36. Mitchell IC, Brown TS, Terada LS, Amatruda JF, Nwariaku FE. Effect of vascular cadherin knockdown on zebrafish vasculature during development. *PLoS One.* 2010;5(1):e8807.
37. Nguyen PD, Hollway GE, Sonntag C, et al. Haematopoietic stem cell induction by somite-derived endothelial cells controlled by meox1. *Nature.* 2014;512(7514):314-318.
38. Swiers G, Rode C, Azzoni E, de Bruijn MF. A short history of hemogenic endothelium. *Blood Cells Mol Dis.* 2013;51(4):206-212.
39. Eilken HM, Nishikawa S, Schroeder T. Continuous single-cell imaging of blood generation from haemogenic endothelium. *Nature.* 2009;457(7231):896-900.
40. Sandler VM, Lis R, Liu Y, et al. Reprogramming human endothelial cells to haematopoietic cells requires vascular induction. *Nature.* 2014;511(7509):312-318.
41. Fraser ST, Yamashita J, Jakt LM, et al. In vitro differentiation of mouse embryonic stem cells: hematopoietic and vascular cell types. *Methods Enzymol.* 2003;365:59-72.
42. Kemp HA, Carmany-Rampey A, Moens C. Generating chimeric zebrafish embryos by transplantation. *J Vis Exp.* 2009;17(29):1394.
43. Tam PP, Rossant J. Mouse embryonic chimeras: tools for studying mammalian development. *Development.* 2003;130(25):6155-6163.
44. Liao EC, Trede NS, Ransom D, Zapata A, Kieran M, Zon LI. Non-cell autonomous requirement for the bloodless gene in primitive hematopoiesis of zebrafish. *Development.* 2002;129(3):649-659.
45. Tanaka M, Gertsenstein M, Rossant J, Nagy A. Mash2 acts cell autonomously in mouse spongiotrophoblast development. *Dev Biol.* 1997;190(1):55-65.
46. Morin-Kensicki EM, Faust C, LaMantia C, Magnuson T. Cell and tissue requirements for the gene eed during mouse gastrulation and organogenesis. *Genesis.* 2001;31(4):142-146.